# Searches for Sterile Neutrinos at Future Electron-Proton Colliders

**Oliver Fischer**[*]

*Department of Physics, University of Basel,*
*Klingelbergstr. 82, CH-4056 Basel, Switzerland.*
*E-mail:* oliver.fischer@unibas.ch

**Stefan Antusch**

*Department of Physics, University of Basel,*
*Klingelbergstr. 82, CH-4056 Basel, Switzerland;*

*Max-Planck-Institut für Physik (Werner-Heisenberg-Institut),*
*Föhringer Ring 6, D-80805 München, Germany.*
*E-mail:* stefan.antusch@unibas.ch

Sterile neutrinos are an attractive extension of the Standard Model of elementary particles towards including a mechanism for generating the observed light neutrino masses. We discuss that when an approximate protective "lepton number"-like symmetry is present, the sterile neutrinos can have masses around the electroweak scale and potentially large neutrino Yukawa couplings, which makes them well testable at planned future particle colliders. We systematically discuss the production and decay channels for sterile neutrinos at electron-proton colliders and give a complete list of the leading order signatures for sterile neutrino searches. We highlight several novel search channels and present a first look at the possible sensitivities for the active-sterile mixing parameters and the heavy neutrino masses. We also compare the performance of electron-proton colliders with the ones of proton-proton and electron-positron colliders, and discuss the complementarity of the different collider types.

---

[*]Speaker.

## 1. Introduction

Since the Standard Model (SM) does not give rise to neutrino masses, the observation of neutrino oscillations is evidence for physics beyond the SM (BSM). Such masses can be realized with Yukawa interactions by adding a number of right-handed neutrinos [2, 3, 4, 5], which are neutral with respect to the SM gauge group, and which are referd to as *sterile* neutrinos. Their lack of quantum numbers also allows for mass terms that mix up only the sterile neutrinos, such that the mass matrix for the neutral fermions contains the Dirac-type masses that emerge after breaking of the electroweak symmetry as well as the Majorana-like masses of the sterile neutrinos.

New physics models with sterile neutrinos can address the dark matter (DM) problem, for instance the $\nu$MSM (see e.g. ref. [6, 7] or ref. [8]), they allow for leptogenesis at the GUT scale (see e.g. refs. [9, 10]), or at the lowscale (e.g. refs. [11, 12, 13, 14]), and even for low masses [15, 16, 17]; they account for the light neutrinos' masses and mixings. See e.g. ref. [18] for a review on the phenomenology of sterile neutrinos in the early universe, and ref. [19] for an overview of searches for sterile neutrinos at particle colliders.

Sterile neutrinos can give rise to the light neutrinos masses when their common mass matrix is diagonalized, which is commonly referred to as the type I seesaw mechanism. We recall the "naïve" version of this mechanism (with one active and one sterile neutrino) with a Dirac mass $m_D = |y_\nu| v_{\text{EW}}$, where $y_\nu$ and $v_{\text{EW}}$ are the neutrino Yukawa coupling and the Higgs vacuum expectation value, respectively, and the sterile neutrino mass $M_R$. In the case where $m_D \ll M_R$, the light neutrino mass can be approximated by

$$m_\nu = \frac{1}{2} \frac{v_{\text{EW}}^2 |y_\nu|^2}{M_R}. \tag{1.1}$$

The upper bounds on the light neutrino mass scale can be naturally explained when $M_R \sim M_{\text{GUT}}$, or, alternatively, for tiny values of $|y_\nu|$. We can expand this simplistic picture of the seesaw mechanism to two active and sterile neutrinos. In this case, the Yukawa and Sterile neutrino masses become $2 \times 2$ matrices, for instance

$$Y_\nu = \begin{pmatrix} \mathcal{O}(y_\nu) & 0 \\ 0 & \mathcal{O}(y_\nu) \end{pmatrix}, \qquad M_N = \begin{pmatrix} M_R & 0 \\ 0 & M_R(1+\varepsilon) \end{pmatrix}, \tag{1.2}$$

where the parameter $\varepsilon$ suggestively indicates the possibility of breaking the mass degeneracy first and the second "family" of light and heavy neutrino mass eigenstates:

$$m_{\nu_i} \approx \frac{v_{\text{EW}}^2 \mathcal{O}(y_\nu^2)}{M_R} (1 - \delta_{i2}\varepsilon). \tag{1.3}$$

Although this scenario allows to explain the observation of the oscillations, also here the upper bounds on the light neutrino mass scale require very large $M_R$ or very small $y_\nu$.

Additional symmetries can give rise to type I seesaw mechanism with large neutrino Yukawa couplings and sterile neutrino masses around the electroweak scale without contradicting the light neutrino masses (cf. ref. [20]). A simple example for such a seesaw scenario with two active and two sterile neutrinos with an additional symmetry is for instance given by

$$Y_\nu = \begin{pmatrix} \mathcal{O}(y_\nu) & 0 \\ \mathcal{O}(y_\nu) & 0 \end{pmatrix}, \qquad \begin{pmatrix} 0 & M_R \\ M_R & \varepsilon \end{pmatrix}, \tag{1.4}$$

with the small parameter $\varepsilon$ breaking the symmetry. In this scenario the light neutrino mass is $m_{\nu_i} \approx 0 + \varepsilon \frac{v_{\mathrm{EW}}^2 \mathscr{O}(y_\nu^2)}{M_R^2}$. Only the perturbation generates a mass (proportional to $\varepsilon$). The bounds on the light neutrino mass scale do not restrict the combination of the neutrino Yukawa coupling and the sterile neutrino mass. This implies, that large neutrino mixings and heavy neutrinos on the electroweak scale can be compatible with the observed smallness of the light neutrino masses.[1]

## 2. The symmetry protected sterile neutrino scenario

As benchmark model we use the Symmetry Protected Seesaw Scenario (the SPSS, see [21]), which does capture the relevant features of seesaw models that feature a symmetry which prevents the light neutrino masses from direct contributions of the neutrino-Yukawa couplings.

The Lagrangian density of the SPSS with its "lepton-number-like" symmetry is given by

$$\mathscr{L} \supset \mathscr{L}_{\mathrm{SM}} - \overline{N_R^1} M N_R^{2c} - y_{\nu_\alpha} \overline{N_R^1} \widetilde{\phi}^\dagger L^\alpha + \mathrm{H.c.} \,, \tag{2.1}$$

where $\mathscr{L}_{\mathrm{SM}}$ contains the SM fields, $L^\alpha$ and $\phi$ denote the lepton and Higgs doublets, respectively, and the kinetic terms of the sterile neutrinos were omitted. Details of the model can be found in ref. [21]. Here important is the definition of the active-sterile mixing parameters, defined as

$$\theta_\alpha = \frac{y_{\nu_\alpha}^*}{\sqrt{2}} \frac{v_{\mathrm{EW}}}{M} \,. \tag{2.2}$$

Also worthy of notice is the fact that the effective mixing matrix of the three active neutrinos, i.e. the Pontecorvo–Maki–Nakagawa–Sakata (PMNS) matrix, is a non-unitary $3 \times 3$ submatrix $\mathscr{N}$ of the $5 \times 5$ leptonic mixing matrix.

### 2.1 Indirect constraints from present precision data

In ref. [22] a bound on active-sterile mixing from a global set of precision observables was extracted. The analysis includes the EWPO, and a list of low energy precision observables:

- Lepton universality observables.
- Lepton flavour violating processes, in particular $\mu \to e\gamma$ (MEG collaboration [23].
- The unitarity of the first row of the CKM matrix.
- The weak mixing angle from the NuTeV experiment, using the recent update in ref. [24].
- Parity violation at energies below the $Z$ boson mass, see e.g. the reviews [25, 26].

The analysis yields upper bounds on active-sterile mixing squared of $\mathscr{O}(10^{-3})$ at 68% ($1\sigma$) Bayesian confidence level (CL)[22]. The resulting constraints on the mixing parameters are included in fig. 1 by the solid, dashed, and dotted lines for $|\theta_e|$, $|\theta_\tau|$, and $|\theta_\mu|$, respectively.

### 2.2 Present constraints from direct searches

Sterile neutrinos have been and are searched for at past end present colliders, respectively. Below is a list with the most stringent limits from searches at LEP and at the LHC.

---

[1]Note that alternatively one can also consider a small perturbation of the structure in eq. (1.4) in the zero elements of $Y_\nu$, and again the generated light neutrino mass(es) are then proportional to this symmetry breaking parameter.
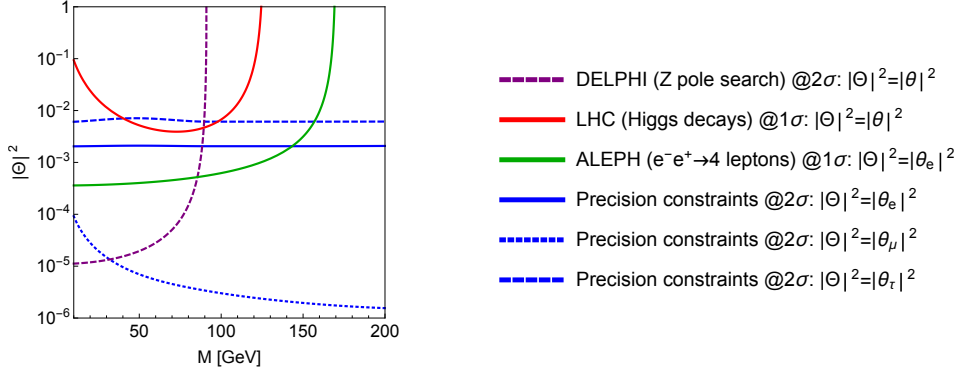
**Figure 1:** Present constraints on the active-sterile mixing parameters from ref. [21].

- Search for sterile neutrinos at the *Z* pole from [27], Opal [28], Aleph [29] and L3 [30], shown by the purple dashed line in fig. 1.
- Modification of the *W* boson production cross section at LEP-II (direct searches have also been performed, e.g. in ref. [31]) shown by the solid green line in fig. 1.
- Modification of the Higgs to diphoton branching ratio shown by the solid red line in fig. 1.

## 3. Heavy neutrino production at $e^- p$ colliders



**Figure 2:** Leading order production channels for heavy neutrinos in electron-proton scattering.

Electron-proton colliders allow for a clean collision environment without pileup at center-of-mass energies of up to a few TeV. Here we consider the LHC upgrade with an electron beam, the Large Hadron-electron Collider (LHeC) [32, 33, 34], and the Future Circular electron-hadron Collider (FCC-eh) [35], which may reuse the electron beam from the LHeC and could yield center-of-mass energies up to 3.5 TeV with comparable luminosities to the LHeC, cf. ref. [36].

At electron-proton colliders heavy neutrinos are produced primarily via $t$-channel exchange of a $W$ boson between electron and parton (called $\mathbf{W_t}^{(q)}$, see fig. 2 left) production channel. Another channel is given by $W\gamma$-fusion (called $\mathbf{W_t}^{(\gamma)}$, see fig. 2 right), which gives rise to a heavy neutrino and a $W^-$ boson. The latter is suppressed by the parton distribution function of the photon, but increasingly important for larger center-of-mass energies and sterile neutrino masses. Both production channels are sensitive on the active-sterile mixing parameter $|\theta_e|$ only.

We show the production cross section $\sigma_N$ divided by $|\theta_e|^2$ for heavy neutrinos via $\mathbf{W_t}^{(q)}$ in fig. 3 at the LHeC (left panel) and the FCC-eh (right panel) for different values of the sterile neutrino mass $M$ as a function of the electron beam energy. The width of the colored bands reflects the impact of the beam polarisation, which increases the cross section up to 80%.

| Name | Final State | $|\theta_\alpha|$ comb. | LFV |
|------|-------------|-------------------------|-----|
| lepton-trijet | $jjj\ell_\alpha^-$ | $\dfrac{|\theta_e\theta_\alpha|^2}{\theta^2}$ | ✓ |
| jet-dilepton | $j\ell_\alpha^-\ell_\beta^+\nu$ | $\dfrac{|\theta_e\theta_\alpha|^{2\,(*)}}{\theta^2}$ | ✓ |
| trijet | $jjj\nu$ | $|\theta_e|^2$ | ✗ |
| monojet | $j\nu\nu\nu$ | $|\theta_e|^2$ | ✗ |

| Name | Final State | $|\theta_\alpha|$ comb. | LFV |
|------|-------------|-------------------------|-----|
| lepton-quadrijet | $jjjj\ell_\alpha^-$ | $\dfrac{|\theta_e\theta_\alpha|^2}{\theta^2}$ | ✓ |
| dilepton-dijet | $\ell_\alpha^-\ell_\beta^+\nu jj$ | $\dfrac{|\theta_e\theta_\alpha|^{2\,(*)}}{\theta^2}$ | ✓ |
| trilepton | $\ell_\alpha^-\ell_\beta^-\ell_\gamma^+\nu\nu$ | $\dfrac{|\theta_e\theta_\alpha|^{2\,(*)}}{\theta^2}$ | ✓ |
| quadrijet | $jjjj\nu$ | $|\theta_e|^2$ | ✗ |
| electron-di-b-jet | $e^-b\bar{b}\nu\nu$ | $|\theta_e|^2$ | ✗ |
| dijet | $jj\nu\nu\nu$ | $|\theta_e|^2$ | ✗ |
| monolepton | $\ell_\alpha^-\nu\nu\nu$ | $|\theta_e|^2$ | ✗ |

**Table 1:** Signatures of sterile neutrinos produced via $\mathbf{W}_t^{(q)}$ (*left* table) and $\mathbf{W}_t^{(\gamma)}$ (*right* table). A checkmark in the "LFV" column indicates that an unambiguous signal for LFV is possible.

In the following we will consider and use electron beam energies of 60 GeV as benchmark, and integrated luminosities of 1 ab$^{-1}$.
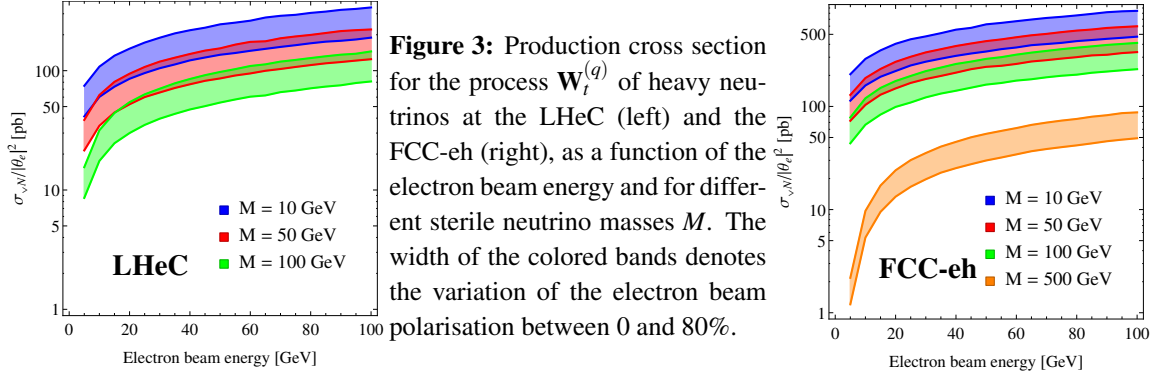


**Figure 3:** Production cross section for the process $\mathbf{W}_t^{(q)}$ of heavy neutrinos at the LHeC (left) and the FCC-eh (right), as a function of the electron beam energy and for different sterile neutrino masses $M$. The width of the colored bands denotes the variation of the electron beam polarisation between 0 and 80%.

### 3.1 Signatures for sterile neutrino searches at $e^- p$ colliders

The most relevant signatures for sterile neutrinos searches at electron-proton colliders were discussed in detail in ref. [19] (for related research, see, e.g., [37, 38]). We refer to heavy neutrino signatures from the $\mathbf{W_t}^{(q)}$ production channel as "four-fermion" final states for the sake of clarity and list their signatures in tab. 1 (left). Analogously, the signatures from the $\mathbf{W_t}^{(\gamma)}$ channel are referred to as "five-fermion" final states, which we list in tab. 1 (right).

The final states without light neutrino, such as the lepton-trijet, allow for unambiguous detection of lepton-flavor violation (LFV). Also the the jet-dilepton final states can give an unambiguous sign of LFV, if the negatively charged lepton is not an electron. Those signatures can in principle also provide an unambiguous sign for lepton number violation (LNV). The signatures in tab. 1 (right) are more relevant at higher center-of-energies and for larger masses $M$. They add further possibilities to search for unambiguous signs of LFV (and also LNV).

### 3.2 First look: lepton-flavour-conserving signatures

The $1\sigma$ parton level ($1\sigma$pl) sensitivities for lepton-number-conserving final states at the LHeC and

e$^-$jjj: $|\Theta|^2 = |\theta_e|^4/|\theta|^2$

$\nu$jjj: $|\Theta|^2 = |\theta_e|^2$

j$\nu\nu$: $|\Theta|^2 = |\theta_e|^2$

e$^-\nu\nu$bb: $|\Theta|^2 = |\theta_e|^2$
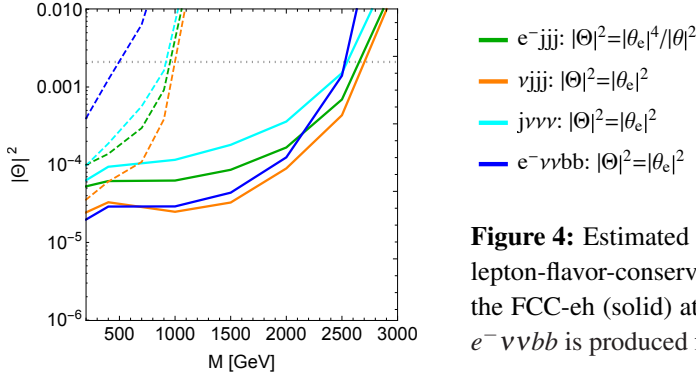
**Figure 4:** Estimated sensitivity for sterile neutrino searches via lepton-flavor-conserving signatures at the LHeC (dashed) and the FCC-eh (solid) at $1\sigma$ from ref. [19]. The blue line labelled $e^-\nu\nu bb$ is produced from the $W\gamma$ fusion channel.

the FCC-eh, obtained in ref. [19], are presented in fig. 4 for the lepton-flavor conserving signatures. In the figure the grey dotted horizontal line denotes the present upper bound on $|\theta_e|$ at the 90% Bayesian confidence level.

The $1\sigma$pl sensitivities for the LFV signatures are shown in fig. 5 for the LHeC (dashed) and the FCC-eh (solid lines). The two black dotted lines denote the present upper bounds on the combinations $|\theta_e\theta_\mu|$ and $|\theta_e\theta_\tau|$ from ref. [22]. The heavy neutrino production cross section is proportional to $|\theta_e|^2$ and the relative strength of the $|\theta_\alpha|^2$ reflects in the relative strength of the lepton flavors. The comparison of figs. 4 and 5 shows that the LFV signatures have better expected sensitivities than the LFC ones. Sterile neutrinos with mixings close to the present upper bound can be tested via the lepton-trijet signature for masses up to $\sim 1$ TeV and $\sim 2.7$ TeV, at the LHeC and FCC-eh, respectively. We note that for $|\theta_\alpha| \sim |\theta_e|$ LFV is something that has to be expected.

The comparison of the LHeC and FCC-eh shows the improves sensitivities from the increased proton beam energy. The relative improvement of the $W\gamma$ fusion signature $e^-\nu\nu bb$ shows that the higher proton beam energy might yield more and competitive signatures.

We remark that, although some of the lepton-number-violating signatures do not have SM backgrounds at the parton level, their cross sections are suppressed by the protective symmetry, and we therefore do not expect the resulting sensitivity to be competitive to the LFV signatures.



$\ell_\alpha^-$jjj ($\alpha = \mu, \tau$): $|\Theta|^2 = |\theta_\alpha\theta_\tau|^2/|\theta|^2$

$\tau^-\mu^+$j$\nu$: $|\Theta|^2 = |\theta_e\theta_\tau|^2/|\theta|^2$
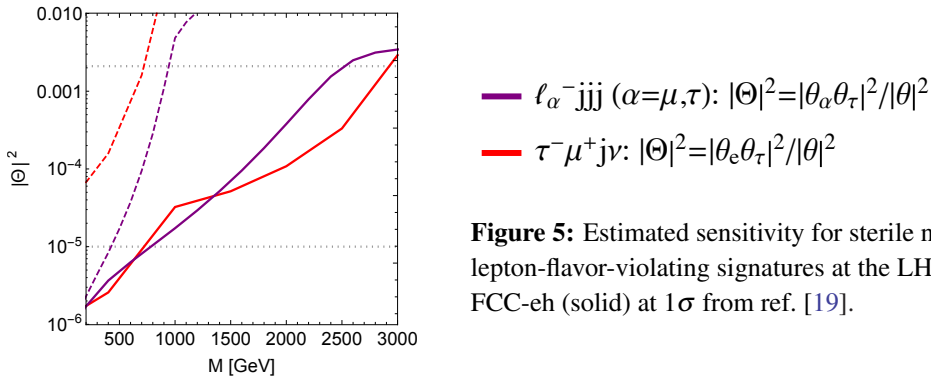
**Figure 5:** Estimated sensitivity for sterile neutrino searches via lepton-flavor-violating signatures at the LHeC (dashed) and the FCC-eh (solid) at $1\sigma$ from ref. [19].

### 3.3 Synergy and Complementarity with other colliders

We show a combination of the different estimated sensitivities for the FCCs, the HL-LHC and the LHeC in fig. 6, see the figure and ref. [19] for details. The $pp$ colliders are shown by the red
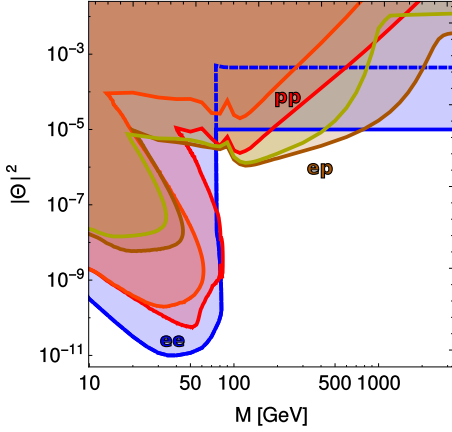
**Figure 6:** Summary of selected estimated sensitivities of the FCC-ee, -hh, and -eh colliders, including the HL-LHC and the LHeC, taken from ref. [19]. The FCC-ee sensitivities of the displaced vertex searches and the sensitivity from the EWPO are shown by the blue lines. Shown in red and dark red are the HL-HLC and the FCC-hh sensitivities, respectively. The estimates for the $e^- p$ colliders, the LHeC in yellow and the FCC-eh in brown have the best prospects for discovering sterile neutrinos via the LFV signatures.

and dark red lines. The best sensitivity from direct searches comes from the searches for LFV lepton-trijets at $e^- p$ colliders, the LHeC and the FCC-eh, shown in yellow and brown, respectively.

## 4. Conclusions

Sterile neutrinos are well motivated extensions of the SM, and symmetry protected seesaw scenarios allow for electroweak scale sterile neutrino masses and $\mathscr{O}(1)$ active-sterile mixings. Present precision data constrain the active-sterile mixing parameters to $|\theta|^2 \leq \mathscr{O}(10^{-3})$.

At electron-proton colliders sterile neutrinos are produced dominantly via the mixing with the electron flavor, $|\theta_e|$. For masses below $m_W$, the best sensitivity can generally be achieved via searches for displaced vertices, which yield sensitivities that are, however, not as good as those at the FCC-ee. The best sensitivity for masses above $m_W$ is expected to come from the lepton-flavor-violating lepton-trijet final state, which could test mixings down to $|\theta_e \theta_\alpha| \sim 10^{-6}$ for both, the LHeC and the FCC-eh.

We emphasize that the sensitivity from direct searches via the lepton-flavor violating signatures at electron-proton colliders significantly enhances the sensitivity of the HL-LHC and the FCC-hh; it can reach smaller values for the active-sterile mixing parameter $|\theta_e|$ or larger values for the masses. In particular, the direct searches for sterile neutrinos can tests sterile neutrinos with masses up to 1.0 and 2.7 TeV at the LHeC and the FCC-eh, respectively.

It is important to realize that the direct searches for sterile neutrinos with masses above a few hundred GeV have greater prospects at electron-proton colliders compared to the proton-proton colliders, and also compared to circular electron-positron colliders. In particular, the improvement of the LHC sensitivity to sterile neutrino searches by the LHeC upgrade is huge. It therefore seems to be a wasted opportunity not to upgrade a proton-proton collider facility with an electron beam.

## References

[1] Figure kindly provided by Marco Drewes, private communication.

[2] P. Minkowski, Phys. Lett. **67B**, 421 (1977).

[3] R. N. Mohapatra and G. Senjanovic, Phys. Rev. Lett. **44**, 912 (1980).

[4] T. Yanagida, Prog. Theor. Phys. **64**, 1103 (1980).

[5] M. Gell-Mann, P. Ramond and R. Slansky, Conf. Proc. C **790927**, 315 (1979) [arXiv:1306.4669 [hep-th]].

[6] L. Canetti, M. Drewes and M. Shaposhnikov, Phys. Rev. Lett. **110**, no. 6, 061801 (2013) [arXiv:1204.3902 [hep-ph]].

[7] L. Canetti, M. Drewes, T. Frossard and M. Shaposhnikov, Phys. Rev. D **87**, 093006 (2013) [arXiv:1208.4607 [hep-ph]].

[8] L. Heurtier and D. Teresi, Phys. Rev. D **94**, no. 12, 125022 (2016) [arXiv:1607.01798 [hep-ph]].

[9] S. Davidson and A. Ibarra, Phys. Lett. B **535**, 25 (2002) [hep-ph/0202239].

[10] T. Hambye, Y. Lin, A. Notari, M. Papucci and A. Strumia, Nucl. Phys. B **695**, 169 (2004) [hep-ph/0312203].

[11] A. Pilaftsis, Phys. Rev. D **56**, 5431 (1997) [hep-ph/9707235].

[12] A. Pilaftsis and T. E. J. Underwood, Nucl. Phys. B **692**, 303 (2004) [hep-ph/0309342].

[13] P. S. Bhupal Dev, P. Millington, A. Pilaftsis and D. Teresi, Nucl. Phys. B **886**, 569 (2014) [arXiv:1404.1003 [hep-ph]].

[14] T. Hambye and D. Teresi, Phys. Rev. Lett. **117**, no. 9, 091801 (2016) [arXiv:1606.00017 [hep-ph]].

[15] M. Drewes and B. Garbrecht, JHEP **1303**, 096 (2013) [arXiv:1206.5537 [hep-ph]].

[16] M. Drewes, B. Garbrecht, D. Gueter and J. Klaric, JHEP **1612**, 150 (2016) [arXiv:1606.06690 [hep-ph]].

[17] M. Drewes, B. Garbrecht, D. Gueter and J. Klaric, JHEP **1708**, 018 (2017) [arXiv:1609.09069 [hep-ph]].

[18] M. Drewes, Int. J. Mod. Phys. E **22**, 1330019 (2013) [arXiv:1303.6912 [hep-ph]].

[19] S. Antusch, E. Cazzato and O. Fischer, Int. J. Mod. Phys. A **32**, no. 14, 1750078 (2017) [arXiv:1612.02728 [hep-ph]].

[20] M. B. Gavela, T. Hambye, D. Hernandez and P. Hernandez, JHEP **0909**, 038 (2009) [arXiv:0906.1461 [hep-ph]].

[21] S. Antusch and O. Fischer, JHEP **1505**, 053 (2015) [arXiv:1502.05915 [hep-ph]].

[22] S. Antusch and O. Fischer, JHEP **1410**, 094 (2014) [arXiv:1407.6607 [hep-ph]].

[23] J. Adam *et al.* [MEG Collaboration], Phys. Rev. Lett. **110**, 201801 (2013) [arXiv:1303.0754 [hep-ex]].

[24] W. Bentz, I. C. Cloet, J. T. Londergan and A. W. Thomas, Phys. Lett. B **693**, 462 (2010) [arXiv:0908.3198 [nucl-th]].

[25] J. Erler and M. J. Ramsey-Musolf, Prog. Part. Nucl. Phys. **54**, 351 (2005) [hep-ph/0404291].

[26] K. S. Kumar, S. Mantry, W. J. Marciano and P. A. Souder, Ann. Rev. Nucl. Part. Sci. **63**, 237 (2013) [arXiv:1302.6263 [hep-ex]].

[27] P. Abreu *et al.* [DELPHI Collaboration], Z. Phys. C **74**, 57 (1997) Erratum: [Z. Phys. C **75**, 580 (1997)].

[28] M. Z. Akrawy *et al.* [OPAL Collaboration], Phys. Lett. B **247**, 448 (1990).

[29] D. Decamp *et al.* [ALEPH Collaboration], Phys. Rept. **216**, 253 (1992).

[30] O. Adriani *et al.* [L3 Collaboration], Phys. Rept. **236**, 1 (1993).

[31] P. Achard *et al.* [L3 Collaboration], Phys. Lett. B **517**, 67 (2001) [hep-ex/0107014].

[32] M. Klein, arXiv:0908.2877 [hep-ex].

[33] J. L. Abelleira Fernandez *et al.* [LHeC Study Group], J. Phys. G **39**, 075001 (2012) [arXiv:1206.2913 [physics.acc-ph]].

[34] O. Bruening and M. Klein, Mod. Phys. Lett. A **28**, no. 16, 1330011 (2013) [arXiv:1305.2090 [physics.acc-ph]].

[35] F. Zimmermann, M. Benedikt, D. Schulte and J. Wenninger, IPAC-2014-MOXAA01.

[36] M. Klein, Annalen Phys. **528**, 138 (2016).

[37] F. S. Queiroz, Phys. Rev. D **93** (2016) no.11, 118701.

[38] M. Lindner, F. S. Queiroz, W. Rodejohann and C. E. Yaguna, JHEP **1606** (2016) 140 [arXiv:1604.08596 [hep-ph]].

PoS(DIS2017)090